

SPIN DISTRIBUTION OF FISSION FRAGMENTS INVOLVING BENDING AND WRIGGLING MODES

D.E. Lyubashevsky,^{1,2,*} A.A. Pisklyukov,¹ D.A. Stepanov,¹ T.Yu. Shashkina,¹ and P.V. Kostryukov^{3,1}

¹*Voronezh State University, Voronezh, Russia*

²*International Institute of Computer Technologies, Voronezh, Russia*

³*Voronezh State University of Forestry and Technologies, Voronezh, Russia*

(Dated: December 6, 2024)

This paper presents a theoretical description of the spin distributions of fragments from low-energy induced and spontaneous nuclear fission, expressed in an analytical form. The mechanism of pumping high spin values for deformed fission fragments is explained. The idea is that the source of the generation of high relative orbital moments and spins of the fragments are the transverse wriggling and bending oscillations of the pre-fragments, while the nucleus remains “cold” until the moment of fission. To verify this hypothesis, experimental distributions for the induced fission of ^{232}Th and ^{238}U nuclei, as well as the spontaneous fission of ^{252}Cf , were compared. The results show reasonable agreement both in the magnitude of the mean spin values and in the sawtooth shape of the spin distribution with respect to the fragment mass number. The results are also compared with other approaches to the description of these quantities, and possible reasons for their discrepancies are discussed.

Keywords: spin distribution; bending and wriggling modes; cold fissioning nucleus; momentum representation

I. INTRODUCTION

In quantum fission theory [1–4], characteristics such as multiplicities, energy and angular distributions of evaporation and delayed neutrons or γ -quanta [5, 6] are closely related [7, 8] to the spin distributions of primary fission fragments (PFF). Empirical data show that the spin values J_1 and J_2 significantly exceed the spin of the compound nucleus J_0 . This is explained [5, 6] by the perpendicular orientation of the vectors \mathbf{J}_1 and \mathbf{J}_2 relative to the symmetry axis of the fissioning nucleus at the moment of its rupture into PFF. However, the mechanism of pumping to such high spin values remains controversial.

An attempt to explain this phenomenon by the Coulomb interaction of highly deformed fission fragments proved unsatisfactory. As shown in [9], this interaction can only change the spins of the fragments \mathbf{J}_1 and \mathbf{J}_2 by small amounts $\Delta J_1, \Delta J_2 \leq 2$, which is incomparable with the average values $J_1, J_2 \gtrsim 6$.

The modern understanding of the phenomenon is based [5, 6, 8–12] on the usage of collective vibrational modes of the fissioning nucleus near its scission point. These modes are usually classified [13] into six types: longitudinal tilting and twisting oscillations, in which the pre-fragments rotate around the symmetry axis of the nucleus Z , and transverse [14] wriggling and bending oscillations, in which the pre-fragments rotate relative to an axis perpendicular to Z . The latter two types of oscillations [15] provide the largest contribution to the spin values of the PFF due to the significant difference in relaxation times for longitudinal and transverse modes. For transverse modes, relaxation rates are faster, making their excitation more likely.

In bending oscillations, the pre-fragments are rotating in opposite directions, and by the law of conservation of total angular momentum, the spins must satisfy the condition $\mathbf{J}_{1b} = -\mathbf{J}_{2b}$. In wriggling oscillations, both pre-fragments rotate in the same direction, resulting in a total spin $\mathbf{J}_w = \mathbf{J}_{1w} + \mathbf{J}_{2w}$, compensated by the rotation of the whole system in the opposite direction, resulting in a relative orbital moment \mathbf{L}_w , related to \mathbf{F}_w by the equality $\mathbf{L}_w = -\mathbf{J}_w$. The proportions of the contributions of these modes to the spin pumping remain unclear. Previously [5, 9, 10], it was assumed that bending mode play the major role in the formation of the spin distributions of the PFF. However, a variety of theoretical works [15–17] show a comparable contribution of both types of oscillations.

Uncertainties in the description of nuclear fission are caused both by the complexity of describing the processes occurring near the scission point of the nucleus and by the lack of experimental data on the spin distributions. In a recently published paper [18], the spins of secondary fission fragments (SFF) were measured in reactions of low-energy induced and spontaneous fission of ^{232}Th , ^{238}U , and ^{252}Cf nuclei. These data allowed the theoreticians to test their models, two of which stand out and are being actively developed by leading research groups.

The studies of the first group are based on the phenomenological FREYA model [19], which uses a statistical approach to describe nuclear processes. The contribution of wriggling and bending oscillations is taken into account [15–17] during thermalization (emission of γ -quanta and neutrons), after which the PFF transitions to secondary fragments. For ^{238}U and ^{252}Cf , the calculations of the SFF spins according to this model are in good agreement [17] with the mentioned experimental data [18].

The second approach [20–22] uses time-dependent den-

* lyubashevskiy@phys.vsu.ru

sity functional theory (TDDFT). It is based [22] on the principles of Fermi’s Golden Rule: the probability of transition from the initial state to the final state is proportional to the square of the average matrix element and the density of the final states. In addition to wriggling and bending oscillations, the model introduces longitudinal tilting and twisting oscillations, allowing the spin to be described in three-dimensional space. Calculations have shown angular distribution changes that differ from the FREYA model [17] and show a clear maximum at an angle of $\frac{2}{3}\pi$. This result is also confirmed by the antisymmetric molecular dynamics method of the Chiba group [23], although in this case the maximum shifts closer to the angle $\frac{\pi}{2}$.

However, both models show a strong correlation between the spins, which contradicts the empirical data [18], as noted in [24]. Also, TDDFT calculations can give erroneous results due to a lack of experimental data [22], and models like FREYA rely on a large number of parameters which rarely have high accuracy.

At present, fission theories do not provide an accurate approach for describing the spin distributions of PFFs outside the framework of the statistical approach and without taking temperature into account. The purpose of this work is to fill this gap using methods of quantum fission theory [1–4], based on the concepts of a “cold” fission nucleus and transitional fission states introduced by O. Bohr [25]. It is shown that the use of only zero bending and wriggling oscillations is sufficient to obtain distributions in agreement with recent experimental data.

This paper is organized as follows: in the second section, an analysis of the stages of the nuclear fission process is presented and an analytical formula for the spin distributions of the PFF is derived, taking into account the influence of the mentioned oscillation modes. The model is then verified by comparison with experimental data for the induced fission of ^{238}U [18]. The third section discusses, in contrast to other theoretical approaches [15, 21], the dependence of the average spin value of PFF on the mass number as an example. The conclusion presents the main results of the study.

II. CONSTRUCTION OF SPIN DISTRIBUTIONS OF PRIMARY FISSION FRAGMENTS

Before proceeding to the description of spin distributions, it is necessary to recall the key stages through which the nucleus passes during low-energy induced and spontaneous fission. These stages play an important role in the formation of the characteristics of PFFs, including their spins, and help to understand the basic mechanisms of the process.

A. Stages of low-energy induced and spontaneous nuclear fission

The initial stage of low-energy induced fission is associated with the capture of a thermal neutron with kinetic energy $T_n \leq 0.025$ eV by the nucleus (A, Z) . This leads to the formation of an excited compound nucleus with energy $E^*(A + 1, Z) \approx |B_n|$, where $B_n \approx -6$ MeV is the neutron binding energy for the nucleus $(A + 1, Z)$ in the ground state. Within nuclear times $\tau_{nuc} \sim 10^{-21}$ s, this excited state transitions to a resonance state, whose wave function Ψ_K^{JM} in the framework of Wigner’s random matrix method [1, 26–28] has the form:

$$\Psi_K^{JM} = b_0 \psi_{0K}^{JM}(\beta_\lambda) + \sum_{i \neq 0} b_i \psi_{iK}^{JM}. \quad (1)$$

Here, the function ψ_{iK}^{JM} describes the i -quasiparticle excited state of the nucleus, and $\psi_{0K}^{JM}(\beta_\lambda)$ describes the collective deformation motion of the nucleus with excitation energy $|B_n|$, which corresponds to the transitional fission state [25]. The coefficients b_i obey the Wigner distribution [26–28], and their squares have mean values $\bar{b}_i^2 = 1/N$, where $N \approx 10^6$ is the total number of quasiparticle states involved in the formation of Ψ_K^{JM} (1).

The evolution of the wave function ψ_{0K}^{JM} is determined by the potential V , which depends on the deformation parameter β_λ . In the generalized liquid-drop model of the nucleus, taking into account shell corrections [29], the potential is represented by a double-humped barrier, schematically shown in Fig. 1.

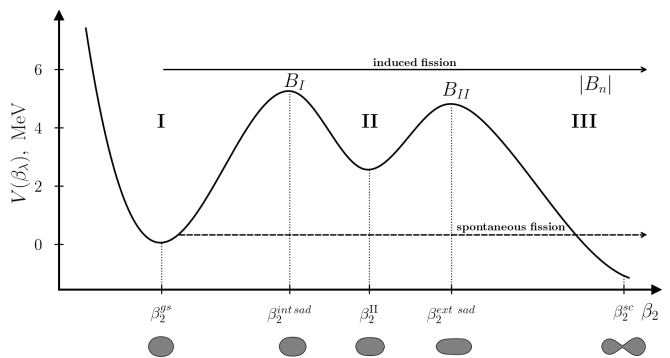


Figure 1. Basic scheme of the potential V depending on the quadrupole deformation of the nucleus β_2 . The region I corresponds to the ground state of the nucleus with β_2^{gs} , II to the isomeric states, and III to the out-of-barrier region where the nucleus tends to splitting into PFFs

In induced fission, the excitation $E^* = |B_n|$ exceeds the heights of the fission barriers B_I and B_{II} , allowing collective deformation states with wave functions ψ_{0K}^{JM} to overcome B_{II} and split the nucleus into PFF. These fragments are [3] in “cold” collective deformation states, not thermalized by the deformation parameter. After fission process over time τ_{nuc} , thermalization occurs and the emission of light particles begins: neutrons and γ -quanta.

Spontaneous fission can be described similarly, but without the excitation energy $|B_n|$. For actinide nuclei, it is usually observed when the fissioning nucleus (A, Z) is even-even, in the ground state with total spin J and its projections M, K equal to zero, and is described by the collective deformation wave function ψ_0^{JM} , corresponding to zero deformation oscillations of the nucleus and corresponding to the transitional fission state of this nucleus introduced in [25]. Thus, the nucleus passes the barriers B_I and B_{II} only after reaching the deformations β_2^{int} and β_2^{ext} . The mentioned transitional fission state changes through potential deformation barriers into the pre-fission configuration shown in Fig. 1.

B. Role of transverse bending and wriggling oscillations in the spin distributions of PFF

Approaching the scission point of the nucleus, as mentioned in the section I, the pre-fragments undergo different vibrational modes, leading to the pumping of the spins of the PFF. Since the fissioning nucleus remains “cold” until the moment of rupture, bending and wriggling oscillations play the main role. Then, according to [14], the spin distribution density function can be represented as the product of the probability density functions of these two independent modes, which have a form similar to the normal distribution. The exponent is dimensionless and the energy of the oscillations is measured in MeV. In this case, the probability distribution can be written as

$$P(J_{k_x}, J_{k_y}) = P(J_{k_x})P(J_{k_y}) = \frac{1}{\pi I_k \hbar \omega_{0_k}} \exp \left[-\frac{J_{k_x}^2 + J_{k_y}^2}{I_k \hbar \omega_{0_k}} \right], \quad (2)$$

where the index $k = w, b$ corresponds to wriggling or bending oscillations, I_k is the moment of inertia of these modes. In the following we will use the parameter C_k , which is the product of the quantities $I_k \hbar \omega_{0_k}$. The frequency ω_{0_k} is determined by the classical formula

$$\omega_{0_k} = \sqrt{\frac{K_k}{I_k}},$$

where K_k is the stiffness coefficient of the corresponding oscillations [14], and I_k is the moment of inertia of the given type of vibration.

Calculating the values of the frequencies for each pair of PFFs is a non-trivial task. We used the results of [10], which attempted to solve this problem for the case of bending oscillations in the spontaneous fission of ^{252}Cf . Since a wide range of experimental data was not yet available at the time of the calculation, the authors of [10] estimated the frequencies for only 8 pairs of PFFs, not 31 as in the paper [18]. Nevertheless, the mass-number range for the light fragment was in the region [100, 120] and for the heavy fragment in the region [132, 152], almost completely covering the range we are investigating.

According to [10] there is a linear dependence of the frequencies of the oscillations on the mass number of the fragment A_f in these regions. Therefore, we believe it is reasonable to estimate the values for the missing pairs using the method of maximum likelihood.

Unfortunately, similar values could not be found for the other two nuclei considered in [18], ^{232}Th and ^{238}U . Therefore, two hypotheses have been proposed. The first is related to the estimation of the bending vibration frequencies ω_b for the mentioned nuclei, which, in the framework of a qualitative estimation, should not differ significantly from the analogous frequencies in the case of spontaneous fission of ^{252}Cf . The second assumes that the values of ω_b for these cases will be close to the analogous values of the same pairs, as for the reaction $^{252}\text{Cf}(\text{sf})$. Strictly speaking, this is not quite correct, at least because of the different stiffness coefficients K and mass number of the compound nucleus A , as well as differences in the fission mechanisms. However, this is mitigated by the use of the concept of “coldness” of fission.

In this case, one can take as a basis the concept of Nix’s work [14], in which an analysis was performed and relations between the frequencies of the wriggling and bending oscillations were established for $^{252}\text{Cf}(\text{sf})$: $\omega_w = 2.6\omega_b$, and for the induced fission of ^{232}Th and ^{238}U nuclei: $\omega_w = 2.5\omega_b$. Of course, we assume that the values of ω_b may differ from those used, but the order of their deviation will be 0.1 MeV, which can be neglected in the first approximation. The results of the frequency estimates of the aforementioned modes are presented in Tables I–III.

The next important step is to describe the moments of inertia of wriggling or bending oscillations. In the case of first one, the magnitude of the moment of inertia I_w , described in the works [15–17], is calculated as follows

$$I_w = \frac{I_0}{I} (I_1 + I_2), \quad (3)$$

where I_i are the moments of inertia of the i -th PFF, $I_0 = \frac{M_1 M_2}{M_1 + M_2} (R_1 + R_2 + d)^2$ is the moment of inertia of the fissile nucleus, $d = 4$ fm is the diameter of its neck; $I = I_0 + I_1 + I_2$ is the total moment of inertia. It is known that the moment of inertia of a solid can be written as $I_i \equiv I_{i, \text{rigid}} = \frac{M_i}{5} \sum R_i^2$, where M_i is the mass of the i -th PFF, and the value R_i depends on the quadrupole deformation parameter β_{2_i} as follows

$$R_i(\beta_{2_i}) = r_0 A^{1/3} \left[1 - \beta_{2_i}^2 / 4\pi + \beta_{2_i} \sqrt{5/4\pi} \right].$$

However, the moments of inertia I_i within the framework of the superfluid model of the nucleus, as proposed by Migdal [30], exhibit notable discrepancies from their solid-body analogs. A more detailed construction of the moments of inertia of PFF and their study was described in detail in [31]. Here, we will merely note that during the calculations, the following ranges of values were obtained for nuclei that were far from “magic” nuclei: $I_i = 0.5 - 0.7 I_{\text{rigid}}$, and for the case of nuclei near “magic” nuclei: $I_i = 0.1 - 0.3 I_{\text{rigid}}$.

Table I. Average spin values calculated using formula Eq. (13) and related parameters of PFF for $^{238}\text{U}(n, f)$

$A_1 X_1$	$A_2 X_2$	β_{2_1}	β_{2_2}	$I_b, \hbar^2/\text{MeV}$	$I_w, \hbar^2/\text{MeV}$	I_1/I_{rigid}	I_2/I_{rigid}	$\hbar\omega_b, \text{MeV}$	\bar{J}_1, \hbar	\bar{J}_2, \hbar
^{82}Ge	^{157}Nd	0.372	0.723	39.79	41.77	0.10	0.55	0.7	4.69	8.56
^{84}Se	^{155}Ce	0.516	0.622	38.93	41.06	0.10	0.55	0.7	4.65	8.46
^{86}Se	^{153}Ce	0.527	0.702	43.23	49.32	0.28	0.64	0.7	5.02	8.63
^{88}Se	^{151}Ce	0.536	0.690	41.30	50.48	0.42	0.62	0.7	5.09	8.13
^{88}Kr	^{151}Ba	0.533	0.663	40.53	45.68	0.24	0.60	0.7	4.80	8.33
^{90}Kr	^{149}Ba	0.561	0.660	27.49	38.39	0.42	0.40	0.7	4.46	6.31
^{92}Kr	^{147}Ba	0.602	0.650	26.30	39.34	0.47	0.40	0.8	4.92	6.45
^{94}Kr	^{145}Ba	0.632	0.637	31.70	46.80	0.53	0.50	0.8	5.37	7.06
^{94}Sr	^{145}Te	0.627	0.588	31.09	45.99	0.53	0.50	0.8	5.34	7.08
^{96}Sr	^{143}Xe	0.659	0.594	31.04	47.54	0.55	0.50	0.85	5.63	7.08
^{98}Sr	^{141}Xe	0.676	0.587	30.17	48.29	0.58	0.50	0.91	5.93	7.03
^{98}Zr	^{141}Xe	0.688	0.563	29.82	48.5	0.60	0.50	0.9	5.18	7.01
^{100}Zr	^{139}Te	0.686	0.555	20.68	43.68	0.68	0.35	0.9	6.19	5.32
^{102}Zr	^{137}Te	0.717	0.546	17.03	44.34	0.77	0.30	0.9	6.67	4.64
^{104}Zr	^{135}Te	0.754	0.530	16.53	45.57	0.79	0.30	0.9	6.86	4.53
^{102}Mo	^{137}Sn	0.712	0.551	16.98	35.85	0.65	0.30	0.9	6.11	4.79
^{104}Mo	^{135}Sn	0.776	0.510	16.59	41.75	0.68	0.30	0.9	6.33	4.64
^{130}Sn	^{109}Mo	0.452	0.758	12.02	35.17	0.20	0.60	1	3.66	6.29
^{132}Sn	^{107}Mo	0.470	0.754	12.26	34.59	0.20	0.60	1	3.94	6.56
^{134}Sn	^{105}Mo	0.503	0.791	12.03	34.55	0.20	0.60	1	4.03	6.50
^{132}Te	^{103}Zr	0.487	0.741	12.38	38.53	0.20	0.70	1	3.86	7.09
^{134}Te	^{105}Zr	0.522	0.757	12.74	34.44	0.20	0.60	1	4.03	6.50
^{136}Te	^{103}Zr	0.536	0.733	19.25	42.21	0.30	0.70	0.9	4.84	6.51
^{138}Te	^{101}Zr	0.543	0.702	19.69	38.44	0.30	0.60	0.9	5.11	5.99
^{138}Xe	^{101}Sr	0.565	0.679	19.60	38.35	0.30	0.60	0.9	5.10	5.97
^{140}Xe	^{99}Sr	0.582	0.672	32.14	46.91	0.50	0.55	0.9	7.22	6.00
^{142}Xe	^{97}Sr	0.593	0.671	32.82	45.82	0.50	0.50	0.85	7.26	5.63
^{142}Ba	^{97}Kr	0.616	0.649	32.67	44.63	0.50	0.50	0.85	7.25	5.63
^{144}Ba	^{95}Kr	0.620	0.639	33.19	46.95	0.50	0.50	0.8	7.18	5.38
^{146}Ba	^{93}Kr	0.620	0.592	32.80	40.66	0.50	0.50	0.8	7.30	5.29
^{148}Ba	^{91}Kr	0.659	0.580	33.02	43.67	0.50	0.40	0.7	7.14	4.67
^{148}Ce	^{91}Se	0.680	0.569	33.19	43.79	0.50	0.40	0.7	7.12	4.70
^{150}Ce	^{89}Se	0.684	0.552	41.90	51.96	0.64	0.40	0.7	8.26	5.07

In the works [15–17], the moment of inertia of bending oscillations I_b differs significantly from the analogous values obtained in [10, 14, 32] and is determined as

$$I_b = \frac{I_1 I_2}{I_1 + I_2}. \quad (4)$$

In the absence of a definitive physical justification for this definition within the previously referenced works, we will adopt the definition of I_b presented in [32] as

$$I_b = \frac{\mu R^2 I_H}{\mu R^2 + I_H}, \quad (5)$$

where $\mu = \frac{M_1 M_2}{M_1 + M_2}$ is the reduced mass, and I_H is the

moment of inertia of the heavy fragment.

The results of the estimation of the moments of inertia of the vibrational and bending modes calculated according to Eqs. (3) and (5) for the fission reactions of $^{232}\text{Th}(n, f)$ and $^{238}\text{U}(n, f)$ as well as $^{252}\text{Cf}(sf)$ are given in Tables I–III.

We will establish the relationship between the projections of the spins of wriggling and bending oscillations $J_{k_p}(p = (x, y))$, through the projections of the spins \mathbf{J}_i on the X and Y axes, perpendicular to the Z axis. For this, we will use formulas similar to those proposed in the works [15–17] and express the spins \mathbf{J}_i through the spins of the mentioned oscillations \mathbf{J}_k , then the contribution

Table II. Average spin values calculated using formula Eq. (13) and related parameters of PFF for $^{232}\text{Th}(n, f)$

$A_1 X_1$	$A_2 X_2$	β_{2_1}	β_{2_2}	$I_b, \hbar^2/\text{MeV}$	$I_w, \hbar^2/\text{MeV}$	I_1/I_{rigid}	I_2/I_{rigid}	$\hbar\omega_b, \text{MeV}$	\bar{J}_1, \hbar	\bar{J}_2, \hbar
^{82}Ge	^{151}Ce	0.392	0.654	36.75	39.83	0.10	0.55	0.70	4.52	8.23
^{84}Ge	^{149}Ce	0.418	0.618	36.14	38.34	0.10	0.55	0.70	4.46	8.08
^{84}Se	^{149}Ba	0.415	0.599	36.57	38.72	0.10	0.55	0.70	4.47	8.12
^{86}Se	^{147}Ba	0.437	0.571	32.17	38.64	0.28	0.50	0.70	4.39	7.24
^{88}Se	^{145}Ba	0.482	0.716	34.26	34.30	0.42	0.55	0.70	4.74	7.24
^{88}Kr	^{145}Xe	0.474	0.552	34.26	39.59	0.24	0.55	0.70	4.45	7.59
^{90}Kr	^{143}Xe	0.496	0.526	30.67	41.32	0.42	0.50	0.70	4.60	6.74
^{92}Kr	^{141}Xe	0.52	0.525	29.51	42.51	0.47	0.50	0.80	5.05	6.92
^{94}Kr	^{139}Xe	0.55	0.521	23.38	39.95	0.56	0.40	0.80	5.17	5.71
^{92}Sr	^{141}Te	0.518	0.487	29.40	36.69	0.30	0.50	0.80	4.59	7.31
^{94}Sr	^{139}Te	0.539	0.502	17.82	33.76	0.53	0.30	0.80	4.91	4.84
^{96}Sr	^{137}Te	0.649	0.436	17	37.45	0.64	0.30	0.85	5.64	4.73
^{98}Sr	^{135}Te	0.719	0.454	16.50	35.91	0.58	0.30	0.90	5.65	4.84
^{98}Zr	^{135}Sn	0.731	0.437	16.56	36.51	0.60	0.30	0.90	5.72	4.82
^{100}Zr	^{133}Sn	0.735	0.443	10.94	35.53	0.68	0.20	0.90	6.22	3.58
^{130}Sn	^{103}Zr	0.411	0.774	9.16	30.89	0.15	0.60	1	3.28	6.43
^{132}Sn	^{101}Zr	0.358	0.766	12.41	32.70	0.20	0.60	1	4.00	6.27
^{132}Te	^{101}Sr	0.371	0.740	12.35	32	0.20	0.60	1	4.00	6.25
^{134}Te	^{99}Sr	0.420	0.727	12.59	32	0.30	0.60	0.90	4.97	5.87
^{136}Te	^{97}Sr	0.430	0.68	19.01	36.43	0.30	0.60	0.90	5.07	5.77
^{138}Te	^{95}Sr	0.455	0.627	19.10	35.79	0.30	0.60	0.95	5.01	5.42
^{138}Xe	^{95}Kr	0.473	0.623	19.26	35.99	0.30	0.60	0.85	5.02	5.48
^{140}Xe	^{93}Kr	0.516	0.561	30.69	42.97	0.50	0.50	0.85	7.15	5.38
^{142}Xe	^{91}Kr	0.517	0.514	30.93	43.27	0.50	0.50	0.80	7.09	5.11
^{142}Ba	^{91}Se	0.535	0.507	32.09	43.24	0.50	0.50	0.80	7.08	5.15
^{144}Ba	^{89}Se	0.558	0.491	32.46	41.13	0.50	0.40	0.70	6.91	4.58
^{146}Ba	^{87}Se	0.565	0.459	31.61	41.30	0.50	0.40	0.70	7.02	4.54
^{148}Ce	^{85}Ge	0.594	0.435	35.61	44.73	0.55	0.40	0.70	7.53	4.69
^{150}Ce	^{83}Ge	0.640	0.418	40.70	50.33	0.64	0.40	0.70	8.26	4.87

of wriggling oscillations to the spin of PFF is determined by the ratio of the moments of inertia:

$$J_{i_p} = \frac{I_i}{I_1 + I_2} J_{w_p} + (-1)^{i+1} J_{b_p}. \quad (6)$$

As can easily be seen from Eq. (6), it follows that the projections of the spins of the wriggling oscillations J_{w_p} are determined by the sum of the projections of the spins of PFF, i.e.

$$J_{w_p} = J_{1_p} + J_{2_p}. \quad (7)$$

In a similar manner, the projections of the spins of bending oscillations, designated as J_{b_p} , are defined in accor-

dance with the Eqs. (6) and (7) relations:

$$J_{b_p} = J_{1_p} - \frac{I_1}{I_1 + I_2} J_{w_p} = \frac{I_2 J_{1_p} - I_1 J_{2_p}}{I_1 + I_2}. \quad (8)$$

In the work [33], it was demonstrated that the probability distribution of the spins of two independent wriggling and bending oscillations can be represented as the product of the probability distributions of each of them:

$$P(J_{w_p} J_{b_p}) = P(J_{w_p})P(J_{b_p}). \quad (9)$$

Using Eqs. (6)–(8), we can transition the probability distribution Eq. (9) to a dependence on the projections of the spins of PFF, then we get

Table III. Average spin values calculated using formula Eq. (13) and related parameters of PFF for $^{252}\text{Cf}(sf)$

$A_1 X_1$	$A_2 X_2$	β_{2_1}	β_{2_2}	$I_b, \hbar^2/\text{MeV}$	$I_w, \hbar^2/\text{MeV}$	I_1/I_{rigid}	I_2/I_{rigid}	$\hbar\omega_b, \text{MeV}$	\bar{J}_1, \hbar	\bar{J}_2, \hbar
^{96}Sr	^{156}Nd	0.588	0.892	45.70	62	0.58	0.63	0.80	6.12	8.88
^{98}Sr	^{154}Nd	0.639	0.867	45.20	62.20	0.58	0.64	0.80	6.15	8.79
^{98}Zr	^{154}Ce	0.645	0.864	42.30	59	0.55	0.60	0.90	6.35	9.06
^{100}Zr	^{152}Ce	0.697	0.813	39.20	60.10	0.67	0.56	0.90	6.63	8.35
^{102}Zr	^{150}Ce	0.740	0.759	37	59.50	0.69	0.54	0.90	6.71	7.96
^{104}Zr	^{148}Ce	0.740	0.759	33.30	56.70	0.68	0.50	0.90	6.67	7.44
^{102}Mo	^{150}Ba	0.763	0.715	34.40	51.87	0.53	0.50	0.90	6.09	7.91
^{104}Mo	^{148}Ba	0.775	0.668	33.30	56.10	0.66	0.50	0.90	6.6	7.47
^{106}Mo	^{146}Ba	0.810	0.615	32.29	53.66	0.60	0.50	0.90	6.41	7.4
^{108}Mo	^{144}Ba	0.845	0.604	31.50	49.95	0.50	0.50	0.90	6.07	7.45
^{108}Ru	^{144}Xe	0.900	0.567	31.49	49.93	0.51	0.50	1	6.4	7.85
^{110}Ru	^{142}Xe	0.938	0.559	24.84	47.41	0.70	0.40	1	6.65	6.57
^{112}Ru	^{140}Xe	0.444	0.997	23.94	47.23	0.70	0.40	1.20	7.35	7.00
^{112}Pd	^{140}Te	0.498	0.976	23.94	47.27	0.70	0.40	1.20	7.36	7.00
^{114}Pd	^{138}Te	0.549	0.914	17.25	41.98	0.70	0.30	1.20	7.36	5.62
^{116}Pd	^{136}Te	0.559	0.938	16.85	42.32	0.70	0.30	1.20	7.52	5.51
^{130}Sn	^{122}Cd	0.591	0.865	10.26	27.89	0.20	0.40	1.10	4.15	5.84
^{132}Sn	^{120}Cd	0.604	0.845	11.36	28.97	0.20	0.40	1.10	4.26	6.05
^{134}Sn	^{118}Cd	0.615	0.817	10.45	30.73	0.20	0.50	1.10	4.15	6.22
^{136}Te	^{116}Rd	0.668	0.775	15.80	42.32	0.30	0.70	1.20	5.42	7.45
^{138}Xe	^{114}Rd	0.681	0.763	16.17	41.98	0.30	0.70	1.20	5.53	7.34
^{140}Xe	^{112}Ru	0.759	0.740	21.79	47.23	0.40	0.70	1.20	6.85	7.22
^{142}Xe	^{110}Ru	0.794	0.729	22.32	47.41	0.40	0.70	1	6.42	6.5
^{142}Ba	^{110}Mo	0.857	0.673	25.23	50.25	0.40	0.70	0.90	6.32	6.6
^{144}Ba	^{108}Mo	0.864	0.645	33.55	49.95	0.50	0.50	0.90	7.54	6.19
^{146}Ba	^{106}Mo	0.864	0.645	34.54	53.66	0.50	0.60	0.90	7.51	6.34
^{148}Ce	^{104}Zr	0.794	0.729	35.58	57.39	0.50	0.70	0.90	7.52	6.85
^{150}Ce	^{102}Zr	0.857	0.673	45.36	65.24	0.64	0.70	0.90	8.85	7.01
^{152}Md	^{100}Sr	0.864	0.645	43.22	60.21	0.60	0.60	0.90	8.86	6.59
^{154}Md	^{98}Sr	0.864	0.645	47.90	63.32	0.66	0.58	0.80	8.99	6.28

$$\begin{aligned}
 P(J_{1_x}, J_{2_x}, J_{1_y}, J_{2_y}) &= \frac{1}{\pi^2 C_w C_b} \exp \left[- \left(\frac{J_{w_x}^2 + J_{w_y}^2}{C_w} + \frac{J_{b_x}^2 + J_{b_y}^2}{C_b} \right) \right] \left| \frac{\partial(J_{w_x}, J_{b_x}, J_{w_y}, J_{b_y})}{\partial(J_{1_x}, J_{2_x}, J_{1_y}, J_{2_y})} \right| = \\
 &= \frac{1}{\pi^2 C_w C_b} \exp \left[- \left(\frac{(J_{1_x} + J_{2_x})^2 + (J_{1_y} + J_{2_y})^2}{C_w} - \frac{(I_2 J_{1_x} - I_1 J_{2_x})^2 + (I_2 J_{1_y} - I_1 J_{2_y})^2}{C_b (I_1 + I_2)^2} \right) \right]. \quad (10)
 \end{aligned}$$

We will transform the formula (11) from the Cartesian coordinate system to the spherical coordinate system. Since we are considering a model of two-dimensional spins, the polar angles θ_1 and θ_2 take values of $\pi/2$, and the azimuthal angles φ_1 and φ_2 transform as $\varphi = \varphi_1 - \varphi_2$ and $\varphi' = (\varphi_1 + \varphi_2)/2$. After integration over the angle φ' , which takes values in the range $[0, \pi]$, the formula (11)

takes the form

$$\begin{aligned}
 P(J_1, J_2, \varphi) &= \frac{2J_1 J_2}{\pi C_w C_b} \exp \left[-J_1^2 (\alpha I_2^2 + C_w^{-1}) \right. \\
 &\quad \left. - J_2^2 (\alpha I_1^2 + C_w^{-1}) + 2J_1 J_2 \cos \varphi (\alpha J_1 J_2 - C_w^{-1}) \right], \quad (11)
 \end{aligned}$$

where $\alpha = C_b^{-1} (I_1 + I_2)^{-2}$.

By integrating Eq. (11) over the projection of the spin of one of the PFF, taking values in the range $[0, \infty)$,

and then integrating over the azimuthal angle φ in the interval $[0, \pi]$, one can ascertain the function $P(J_i)$ representing the distribution of the remaining PFF's spin projection.

$$P(J_i) = 2J_i d_i \exp\left[-\frac{J_i^2}{d_i}\right], \quad (12)$$

where $d_i = I_i^2 C_w (I_1 + I_2)^{-2} + C_b$.

It is crucial to highlight that the main advantage of the derived formula (12) is its analytical simplicity, which enables the estimation of spin distributions through an intuitively comprehensible algorithm. In contrast to the TDDFT method presented in the work [34], where the bulky calculations of the angular distribution led to incorrect results. Moreover, it took the authors a considerable amount of time to identify the error and obtain new data; the corrected results [35] have only recently been published. Thus, the simplicity and transparency of our proposed approach are critical factors in evaluating the final result of the study.

C. Analyzing fission fragment spin distribution

We will compare the results obtained by simple analytical formulas Eqs. (11) and (12) with the existing experimental data. For this purpose we will use the data published in the paper [18], where the spin distributions of heavy PFFs resulting from the induced fission of the ^{238}U nucleus were obtained.

The spectrum of measured spins varies from ^{130}Sn to ^{150}Ce and is shown in Fig. 2 as black squares with measurement errors. For each PFF, theoretical curves were also constructed using the current approach, i.e. using the formula Eq. (12) and the parameters presented in Table I. The comparison shows reasonable agreement between the theoretical and experimental spin distributions of PFF. The exceptions are the nuclei ^{130}Sn , ^{132}Sn , ^{132}Te , where the curve does not fall within the error range. It should be noted that the comparison involves experimental data on the spin distributions of secondary fission fragments (SFF), which differ from the primary ones due to the emission of evaporation neutrons and γ -quanta. However, due to the relatively low energy of the fission, the spin values carried away from the PFF are small, even in the case of multiple emission processes of the above-mentioned particles. Therefore, such a comparison remains justified and can help to understand the reasons for the discrepancy with the experimental data.

It is regrettable that the aforementioned experimental work did not present the spin distributions of light PFF. However, using the laws of conservation of charge and mass numbers and Eq. (12), theoretical curves for the specified fragments can be obtained. The resulting calculations are presented in Fig. 2, which may be useful for the collaboration of the researchers involved in the work [18].

III. DISCUSSION

Unfortunately, the spin distributions of heavy SFF presented in Fig. 2 are available only for the $^{238}\text{U}(n, f)$ reaction, and we could not find other similar data. However, the authors of the referenced work [18] were able to measure the average spin values for PFF in both low-energy induced fission of ^{238}U and ^{232}Th , as well as spontaneous fission of ^{252}Cf .

It is easily demonstrated that the analytical form of the quantity \bar{J}_i for any PFF can be constructed by multiplying the spin distribution determined by (12) by the spin and integrating within the range $[0, \infty)$, resulting in

$$\bar{J}_i = \int_0^\infty P(J_i) J_i dJ_i = \int_0^\infty 2J_i^2 d_i e^{-\frac{J_i^2}{d_i}} dJ_i = \frac{1}{2} \sqrt{\frac{\pi}{d_i}}. \quad (13)$$

The results of calculating the average spin values using the formula presented in (13) for each pair of PFF for the $^{238}\text{U}(n, f)$ and $^{232}\text{Th}(n, f)$ and $^{252}\text{Cf}(sf)$ are presented in Tables I–III.

The comparison of the dependencies $\bar{J}(A_f)$ obtained within the framework of our approach and from the experimental data presented [18] are presented in Figs. 4–6. It should be noted that, in addition to data presented Figs. 5 and 6, similar quantities obtained in two other models referenced in the Introduction [17, 22] were included for comparison. From their comparative analysis, it can be seen that our method demonstrates better agreement with the experimental data, accurately reproducing the sawtooth nature of the spin dependence on the mass number, as noted in reference [17], where it was associated with changes in the moments of inertia of PFF. The results of our model align with this conclusion. However, in contrast to the statistical approach of FREYA [17], it does not consider the impact of light particle evaporation.

The fact is that statistical models assume that the nucleus heats up to a temperature of about 1 MeV as it descends from the outer saddle point, which for nuclei with atomic mass $A \approx 240$ implies an excitation energy of more than 20 MeV. In addition to [17], this assumption is widely used in various fission models [36–38], which successfully describe the mass and charge distributions of PFF. On the other hand, high temperature leads to complex multi-quasiparticle states with high energy density, ideal for the manifestation of Coriolis interaction. Uniform statistical mixing of spin projections on the symmetry axis for such states of the fissioning nucleus near the point of its rupture, as shown in [3], leads to the complete disappearance of anisotropies of different P and T parities in the angular distributions of the fission fragments. Since such anisotropies are well established for low-energy fission [25, 39–45], it can be concluded that the nucleus remains in a "cold" state up to the point of rupture, although in a non-equilibrium state with respect to deformation.

It is of particular importance to pay close attention to the issue of accurately estimating the moments of iner-

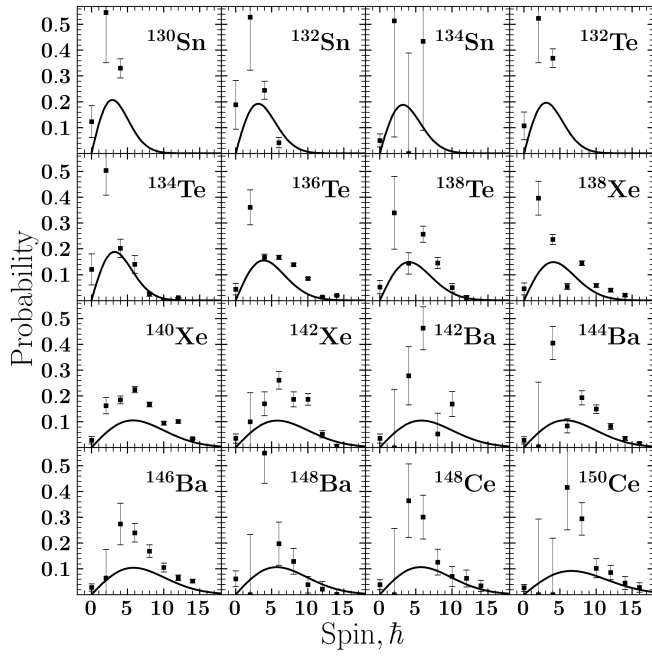


Figure 2. Comparison of the spin distributions of the SFF found in [18] (black squares with errors) and calculated with Eq. (12) (black solid line) for the heavy PFF of $^{238}\text{U}(n, f)$

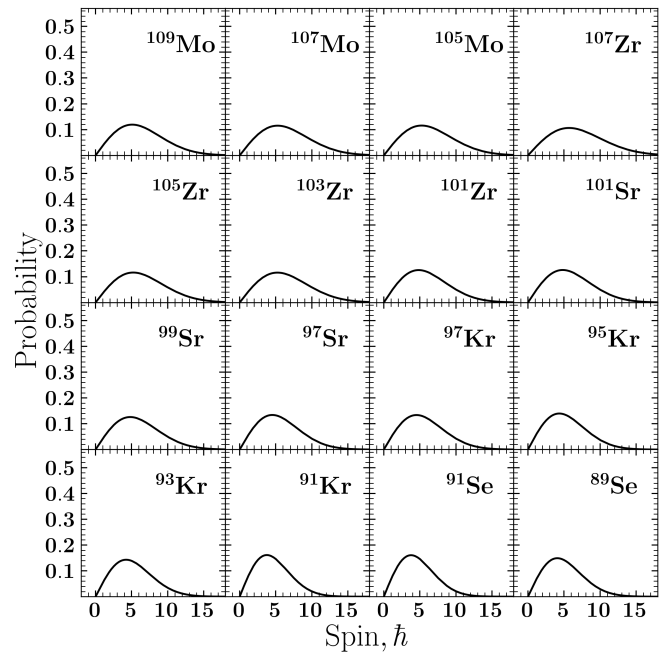


Figure 3. Spin distributions of light PFF of $^{238}\text{U}(n, f)$, calculated using Eq. (12) (black solid line)

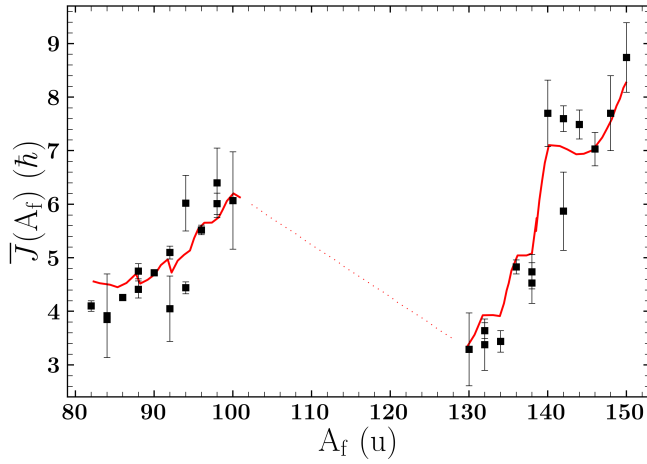


Figure 4. Comparison of the experimental spins of fission fragments, as presented in Ref. [18], and the calculated values by Eq. (13), for the reaction $^{232}\text{Th}(n, f)$. The experimental data, represented by black squares with associated error bars, are shown alongside the calculated values, represented by a red dotted line, in the figure.

tia of the PFF. In the aforementioned work [16], a phenomenological parameterization of the moments of inertia is proposed. This parameterization is based on the “ad hoc” principle and lacks strict physical justification. Concurrently, the precise methodology for determining the moments of inertia is not a crucial concern, according to the authors. Their model incorporates the reduction of the moments of inertia in proximity to magic points

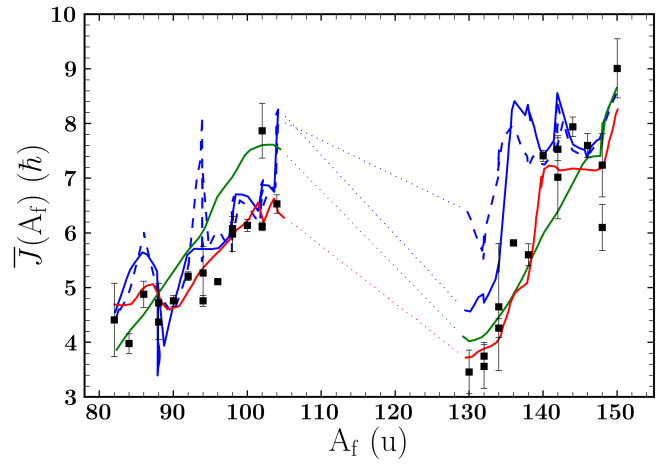


Figure 5. Comparison of the experimental spins of the fragments as presented in Ref. [18] (represented by black squares with associated errors) with the values calculated by Eq. (13) (red dotted line) and the values obtained by theoretical groups for the reaction $^{238}\text{U}(n, f)$ are shown. The values obtained by the Randrup group [17] are represented by a green solid line. The data were obtained by the Bulgak group (blue solid line is the CGMF model and blue dashed line is the CGMF model considering only $2^+ \rightarrow 0^+$ transitions) in Ref. [22].

and, conversely, their growth with distance from these points, which is associated with an increase in the deformation of the PFF. The coefficients in the model were calibrated to achieve comprehensive alignment with the measured spin values presented in [18].

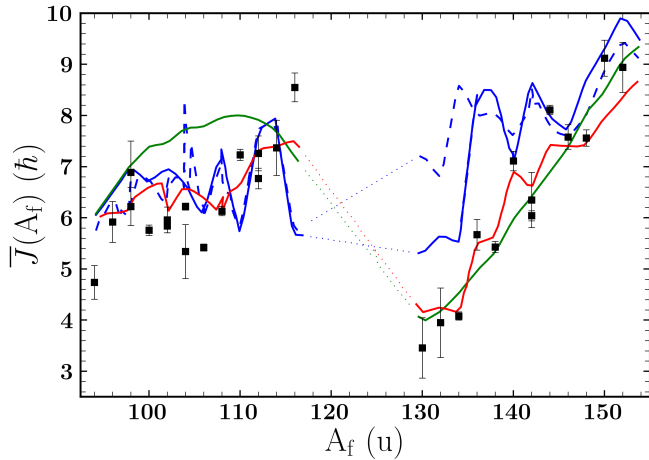


Figure 6. Comparison of the experimental spins of the fragments as presented in Ref. [18] (black squares with errors) with the values calculated by Eq. (13) (red line) with values obtained by other theoretical groups [17, 22] for the reaction $^{252}\text{Cf}(\text{sf})$. The results of the Randrup group are represented by a green solid line, for the Bulgak group – CGMF model (blue line), and CGMF only $2^+ \rightarrow 0^+$ transitions (blue dashed line)

In our approach, it is assumed that the fissioning nucleus remains in a “cold” but non-equilibrium state with regard to its deformation up to the point of rupture. In order to account for this energy, the results of the work [46], which used the example of the nucleus $^{252}\text{Cf}(\text{sf})$, a method for calculating the excitation energy ranging from 5 to 30 MeV was proposed. Such excitation energies arise as a consequence of the transition of PFF from non-equilibrium to equilibrium states with regard to their deformation. Furthermore, fragments in proximity to “magic” nuclei in equilibrium do not exhibit quadrupole deformation, and thus, within the superfluid model proposed by Migdal [30], their moments of inertia approach zero. Given that the pre-fragments are in non-equilibrium states in terms of their deformation for the nuclei before rupture, the moments of inertia calculated in this approach will fall within the range $I_i = 0.1 - 0.3I_{\text{rigid}}$. It is important to note that even for the same PFF but obtained from distinct parent nuclei, the moments of inertia will vary. This is the result of the differing excitation energies of the compound systems.

Furthermore, the deformation of the fragments, which may exhibit significant differences in their moments of inertia compared to those assumed in previous studies, e.g. [15–17], is not incorporated into the calculations based on the FREYA model. This is illustrated in Tables I–III, where the quadrupole deformations β_{2_i} for each of the PFF are given. It can be seen that their equilibrium values significantly differ from zero. Nevertheless, the contribution to the calculated value of the moment of inertia is no more than 30%. This provides further evidence to support the hypothesis that the dis-

crepancy between the results of the work [17] and the experimental data [18] may be attributed to the aforementioned factors.

Moreover, the FREYA model [15–17] selects the spins of the mentioned oscillations J_k from the probability density distribution by the statistical form $P(J_{w,b}) \sim \exp[J_{w,b}^2/(2T_S I_{w,b})]$, where T_S is the effective temperature of the oscillations. The spins of the light J_L and heavy J_H PFF are then determined as

$$J_L = \frac{I_L}{I_0} J_0 + \frac{I_L}{I_w} J_w + J_b, \quad J_H = \frac{I_H}{I_0} J_0 + \frac{I_H}{I_w} J_w - J_b,$$

where I_L and I_H are the moments of inertia of the light and heavy PFF, respectively. It follows that the major contribution to the spins of the light J_L and heavy J_H PFFs comes from the components associated with the wriggling and bending oscillations, since the contribution from the spin ($\bar{J}_0 = 0.36\hbar$) of the parent nucleus can be neglected. The magnitude of the contribution from the wriggling and bending oscillations is determined by the degree of internal excitation during the fission. Since this quantity depends on how much of the total excitation energy (TXE) is associated with the deformation energy, it is not easily accessible and FREYA approximates it using the effective value determined by the expression $c_S^2 TXE = a_0 T_S^2$, where the coefficient c_S is a parameter in FREYA and the level density parameter a_0 is calculated according to the work [47]. Starting from $TXE \approx 22$ MeV for thermal fission, TXE steadily increases and reaches a value of about 40 MeV at $E_n = 20$ MeV, so the effective temperatures of wriggling and bending oscillations T_S are in the range 0.85 – 1.15 MeV. Thus, as shown in the paper [16], the spin values from the contribution of wriggling and bending oscillations are about $4.8\hbar$ and $6.4\hbar$ for the light J_L and heavy J_H PFF, respectively, for fission by thermal neutrons, while at neutron energies $E_n = 20$ MeV the values are $5.8\hbar$ and $7.1\hbar$. Therefore, a key conclusion of the work [16] is the weak dependence of the PFF spin on the energy of the incident neutron over a wide range of energies.

On the other hand, the dynamic TDDFT model [21] better describes the \bar{J} values, albeit with an overestimation for heavy PFF. Unlike the other two theoretical curves, it does not show a sawtooth pattern for the spontaneous fission of ^{252}Cf , which the authors believe is mainly due to the $2^+ \rightarrow 0^+$ transitions. The authors of the papers [20–22, 24] show that at small initial spin values of the parent nucleus $S_0 \approx 0$, the formation of the intrinsic spins of PFF is determined by the predominant contribution of statistical factors, in particular a large number of allowed final intrinsic spin values. The range of allowed intrinsic spin values of PFFs, and in particular their distribution, is determined by their intrinsic deformations. Ultimately, this allowed a reasonable description of the distribution of average spin values for ^{238}U and ^{252}Cf presented in [18]. Within the framework of the consideration of the spin in the three-dimensional case, a distribution of the angle between the spins with the

most probable value equal to $2/3\pi$ was obtained, which is significantly different from the two-dimensional case considered in [16]. This, in turn, imposes serious limitations on the TDDFT method, which can lead to partially erroneous results, as the authors of the paper [21] point out. One of these contradictory facts is that taking into account the three-dimensionality of the spin within the TDDFT method leads [24] to the appearance of correlation coefficients with values close to 1, i.e. to a strong correlation between the spins, which is in direct contradiction with the existing experimental data [18].

Therefore, against the background of such complex models, the simple analytical formulas obtained in this work are a powerful tool for analyzing the spin distributions of PFF. The approach proposed in this work allows a new look at the physics of the fission process, as well as the relationship between quantum and thermodynamic properties of the fission system for different stages of this process. As noted in section II A, the developed approach considers the fission process with low excitation energies through the prism of a mechanism where the nucleus remains “cold” ($T \ll 1$ MeV) during fission. The use of zero bending and wriggling oscillations allows a better reproduction of the average values Figs. 5 and 6 than, for example, the statistical model [15]. Perhaps the use of the average temperature concept does not allow a correct description of the average spins of light fission fragments.

IV. CONCLUSION

In this work, a mechanism for describing the pumping of spins of deformed primary fission fragments (PFF) for the following fission reactions: $^{232}\text{Th}(n, f)$, $^{238}\text{U}(n, f)$, and $^{252}\text{Cf}(sf)$ was proposed. For the first time, analytical formulas for calculating the previously mentioned distri-

butions were obtained. In order to obtain the analytical form, it was necessary to consider the following theoretical approximations: the “coldness” of the fissioning nucleus up to the point of rupture, the law of conservation of total angular momentum, the appearance of large relative orbital moments of the fissioning system, and zero transverse bending and wriggling oscillations. In order to describe these phenomena, the wave functions of the aforementioned vibrational modes of the nucleus in the momentum representation were used. The moments of inertia of the fission fragments were determined within the framework of the superfluid model of the Migdal nucleus, as proposed by Migdal [30], taking into account non-equilibrium deformation.

The calculated spin distributions of PFF within the framework of the proposed theoretical approach are in accordance with the experimental average spin values of low-energy fission. Additionally, the sawtooth-like dependence of the experimentally obtained average spins on the fragment’s mass number can be accurately described. The correlation between the moments of inertia of PFF and the average spin values suggests that measurements of the latter could provide unique insights into the fissioning system during fission. Further refinement of this approach could significantly advance the development of quantum fission theory.

ACKNOWLEDGMENTS

The authors express their gratitude to Professor S.G. Kadomensky for his active engagement in the discussion on the topic of representations of the “coldness” of the fissioning nucleus, as well as to Associate Professor L.V. Titova for her valuable insights and constructive contributions to this work.

-
- [1] S. G. Kadomensky, *Phys. At. Nucl.* **65**, 1785 (2002).
 - [2] S. G. Kadomensky and L. V. Rodionova, *Phys. At. Nucl.* **66**, 1219 (2003).
 - [3] S. G. Kadomensky, *Phys. At. Nucl.* **68**, 1968 (2005).
 - [4] S. G. Kadomensky, *Phys. At. Nucl.* **71**, 1193 (2008).
 - [5] J. B. Wilhelmy *et al.*, *Phys. Rev. C* **5**, 2041 (1972).
 - [6] L. G. Moretto *et al.*, *Nucl. Phys. A* **502**, 453 (1989).
 - [7] K. Skarsvag and K. Bergheim, *Nucl. Phys.* **45**, 721 (1963).
 - [8] A. Gavron, *Phys. Rev. C* **13**, 2562 (1976).
 - [9] J. O. Rasmussen *et al.*, *Nucl. Phys. A* **136**, 465 (1969).
 - [10] T. M. Shneidman *et al.*, *Phys. Rev. C* **65**, 064302 (2002).
 - [11] S. G. Kadomensky *et al.*, *Bull. Russ. Acad. Sci. Phys.* **79**, 879 (2015).
 - [12] V. E. Bunakov *et al.*, *Phys. At. Nucl.* **79**, 304 (2016).
 - [13] T. Døssing and J. Randrup, *Nucl. Phys. A* **433**, 215 (1985).
 - [14] J. R. Nix and W. J. Swiatecki, *Nucl. Phys. A* **71**, 1 (1965).
 - [15] J. Randrup and R. Vogt, *Phys. Rev. Lett.* **127**, 062502 (2021).
 - [16] R. Vogt and J. Randrup, *Phys. Rev. C* **103**, 014610 (2021).
 - [17] J. Randrup *et al.*, *Phys. Rev. C* **106**, 014609 (2022).
 - [18] J. N. Wilson *et al.*, *Nature* **590**, 566 (2021).
 - [19] J. M. Verbeke *et al.*, *Comput. Phys. Commun.* **191**, 178 (2015).
 - [20] A. Bulgac *et al.*, *Phys. Rev. Lett.* **116**, 122504 (2016).
 - [21] I. Stetcu *et al.*, *Phys. Rev. Lett.* **128**, 022501 (2022).
 - [22] A. Bulgac, *Phys. Rev. C* **106**, 014624 (2022).
 - [23] J. Chen *et al.*, *EPJ Web of Conferences* **284**, 04006 (2023).
 - [24] A. Bulgac *et al.*, *Phys. Rev. Lett.* **126**, 142502 (2021).
 - [25] A. Bohr and B. Mottelson, *Nuclear Structure (In 2 Volumes)* (World Scientific Publishing Company, 1998).
 - [26] E. P. Wigner, *Ann. Math.* **62**, 548 (1955).
 - [27] E. P. Wigner, *Ann. Math.* **65**, 203 (1957).
 - [28] E. P. Wigner, *Ann. Math.* **67**, 325 (1958).
 - [29] V. M. Strutinsky, *Nucl. Phys. A* **95**, 420 (1967).
 - [30] A. B. Migdal, *JETP* **37**, 249 (1959).
 - [31] D. E. Lyubashevsky *et al.*, *Chin. Phys. C* **48** (2025).

- [32] T. M. Shneidman *et al.*, *Phys. Rev. C* **92**, 034302 (2015).
- [33] S. G. Kadmsky *et al.*, *Phys. At. Nucl.* **80**, 447 (2017).
- [34] I. Stetcu *et al.*, *Physical Review Letters* **127**, 222502 (2021).
- [35] G. Scamps, *Phys. Rev. C* **109**, L011602 (2024).
- [36] P. Grangé *et al.*, *Phys. Rev. C* **34**, 209 (1986).
- [37] O. Litaize *et al.*, *Eur. Phys. J. A* **51**, 177 (2015).
- [38] K.-H. Schmidt *et al.*, *Nucl. Data Sheets* **131**, 107 (2016).
- [39] U. B. Ostapenko *et al.*, *Sov. JETP Lett.* **12**, 1364 (1981).
- [40] G. A. Petrov *et al.*, *Nucl. Phys. A* **502**, 297 (1989).
- [41] F. Gönnerwein *et al.*, *Nucl. Phys. A* **567**, 303 (1994).
- [42] A. Y. Alexandrovich *et al.*, *Nucl. Phys. A* **567**, 541 (1994).
- [43] P. Jesinger *et al.*, *Nucl. Instrum. Methods Phys. Res. A* **440**, 618 (2000).
- [44] F. Gönnerwein *et al.*, *Int. J. Mod. Phys. E* **16**, 410 (2007).
- [45] A. Gagarski *et al.*, *Phys. Rev. C* **93**, 054619 (2016).
- [46] O. T. Grudzevich, *Problems of Atomic Science and Technology. Series: Nuclear Constants*, 39 (2000).
- [47] J. Randrup and R. Vogt, *Phys. Rev. C* **80**, 024601 (2009).